A Determination of Horizontal Divergence in the Gulf Stream off Cape Lookout

Frank Chew and G. A. Berberian

Atlantic Oceanographic and Meteorological Labs., ESSA, Miami, Fla.

ABSTRACT

A horizontal divergence of 2×10^{-5} sec^{-1} was determined by tracking three shallow drogues in the speed axis of the Gulf Stream. Concurrent bathythermograph soundings along a drogue track support this magnitude. The data also provide estimates of the strength of turbulence encountered. In terms of the neighbor diffusivity, they amount to 2×10^{5} cm^2 sec^{-1} for a drogue separation scale of 4 km, and 4×10^{4} cm^2 sec^{-1} for the 2-km scale.

1. Introduction

The three variables entering the theorem of potential vorticity conservation are the Coriolis parameter f and its latitudinal variation, the horizontal divergence D, and the vertical component of relative vorticity ζ. Of these, D may have the least magnitude as in the discussion by Warren (1963) of topographic meandering where the magnitude of D is of the order of 10^{-7} sec^{-1}. However, in situations where the change in ζ is rapid, we may expect a much larger D. For example, if the order of magnitude of relative vorticity change in one day is that of f, we have $D \approx (1/f)(d\zeta/dt) \approx 10^{-5}$ sec^{-1}. Such changes were envisaged by Newton (1961) and Chew and Berberian (1970). Although the latter represents a 100-fold increase, our ability to measure it directly remains marginal, unless conditions are optimal. This paper reports on a direct determination of local horizontal divergence in the Gulf Stream, together with a discussion of its implication.

2. The measurements

In conjunction with a Gulf Stream study by Richardson *et al.* (1969), four series of drogues were tracked by ESSA personnel on board the ESSA ship *Mt. Mitchell* in the offings of Onslow and Rayleigh Bays in June 1968. However, weather and sea conditions prevented simultaneous location by radar of all drifting drogues except for the final set, when the sea became smooth after the passage of a weather front. The light and variable winds also precluded the occurrence of Ekman divergence as discussed by Niiler (1969). This report is devoted to the last series only.

The 8.5 m diameter parachute drogue was of conventional design; it was attached by a 4 mm ($\frac{5}{32}$ inch) diameter steel cable to a surface float of tire inner tube to which were lashed wooden cross arms supporting an aluminum pole that extended 2.5–3.0 m above the float.

In turn, the pole supported passive radar reflectors, an identifying blinking light, and marks.

The drogues were released in two groups of three each, and tracking was done by visiting and monitoring each drogue in turn for 1 hr while locating the others by radar. For each observation, the sighting of the drogues on radar was recorded manually with simultaneous plotting on the Decca Automatic Radar Plotter; as a further backup, 20 photographs of the radar scope display were taken over a 1-min interval for each observation. When on station, drogue positions were recorded once every 10 min; at the start and end of each drogue visit, a bathythermograph (BT) sounding was made and a surface water sample collected. A thermistor was used to continuously record the temperature of the water at $\sim$2 ft below the sea surface. The accuracy of the radar range reading is ± 200 m, and of azimuth $\pm 2°$; at the range of interest, the latter also amounted to ± 200 m. Navigation control was by Loran A with an accuracy of ± 450 m generally.

3. The data

Initially, two sets of three drogues each at two different depths were tracked. However, two drogues were later lost, presumably from leaks in the inner tubes serving as floatation units. For both original and re-

TABLE 1. Drogue releases and recovery times.

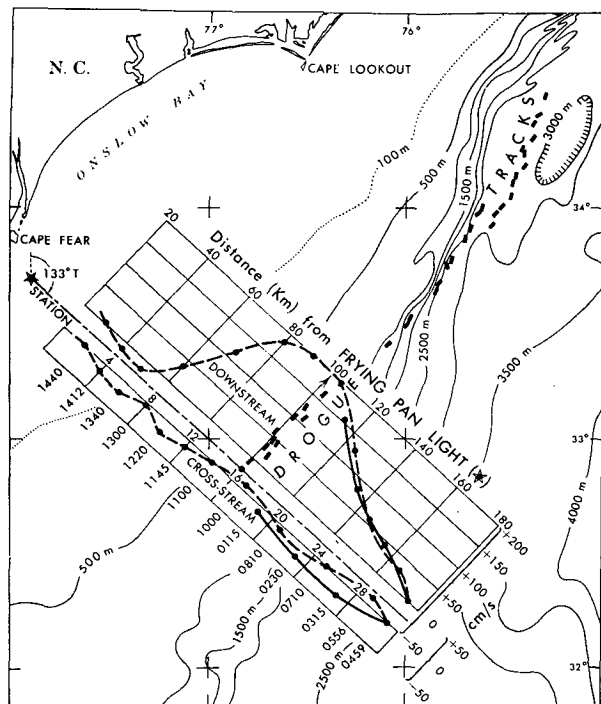| Drogue no.	Release (Date)	(GMT)	Recovery (Date)	(GMT)	Depth of parachute (ft)
10	29 June	1220	30 June	1222	150
11	29 June	1237	lost		150
12	29 June	1255	30 June	1324	150
13	29 June	1628	1 July	0230	65
14	29 June	1654	lost		65
15	29 June	1721	1 July	0330	65
14a	30 June	1806	lost		65

FIG. 1. Drogue tracks and cross-stream profile of surface current in the offings of Cape Fear and Cape Lookout. For drogues, each dash represents a 1-hr track. Surface currents are given in components along compass direction 43° true (downstream) and 133° true (cross stream). Universal time indicates when current was measured on 29 June 1968. Current data were supplied by W. S. Richardson.

placement drogues, Table 1 gives the depths and times of release and recovery.

For their transport measurement, Richardson *et al.* (1969) had selected a section across the stream that started from Frying Pan Light on a course of 133° true, and had, on the day of drogue releases, made the measurement of surface current shown in Fig. 1. All drogues were deployed at station 16 on this section. They are seen to follow nearly straight tracks more or less parallel to shallow bottom contours such as the 100 m isobath, but to cut across the deeper isobaths (1000–2000 m) at a considerable angle.

Fig. 2 presents a plot of the distance traversed by each drogue against time. The slopes of the curves, fitted by eye, give the speeds of the drogues. For all drogues, the initial velocity was 200 ±5 cm sec^{-1} on a weakly anticyclonic path. This compares favorably with Richardson's observation at Station 16 of a downstream speed of 200 cm sec^{-1} and a cross-stream speed of 8 cm sec^{-1} toward deeper water, although the time difference between the two independent sets varied from 2–7 hr. For drogues 13 and 15, in particular, the initial speed was 200 cm sec^{-1}; they then slowed to 160 cm sec^{-1} after 25 hr, but later returned to a somewhat higher speed of 170 cm sec^{-1} toward the end of the observation period.

The beginning and end portions of the paths shown in Fig. 1 are enlarged and illustrated with a procession of triangles in Figs. 3 and 4. The vertices of the successive triangles represent the successive locations of the three drogues located simultaneously by radar. Positive identification, frequent monitoring, and two sets of backup data remove all doubts in the sequence of development shown in the figures, where for clarity of presentation, only about half the data are depicted. The salient features are: 1) the curvature of the paths; 2) the crossing of the paths of drogues 14a and 15; and 3) the rotation, deformation, and change in the size of the triangles. Some measures of these kinematic parameters for the whole series are shown in Fig. 5.

Fig. 6 shows the temperature sections along the paths of drogues 12 and 15, respectively, where all BT soundings were taken by the same instrument and are plotted without correction to facilitate detection of changes. Finally, in Fig. 7 we have plotted against time the natural logarithm of the area of the triangles formed with drogues 13, 14a and 15 as vertices.

4. Turbulence

To help assess the accuracy of horizontal divergence measurements, we shall first consider the horizontal turbulence encountered, utilizing the theory of neighbor diffusivity which states that the neighbor diffusivity F is related to the neighbor separation L by

$$F = BL^{\frac{4}{3}}, \qquad (1)$$

where B is a coefficient whose magnitude is poorly determined, but ranges from 0.001–0.01 when F is in cm^2 sec^{-1} (Okubo, 1962). To avoid this uncertainty, we determined F directly by the method given by Stommel (1949), with the further assumption that the field of
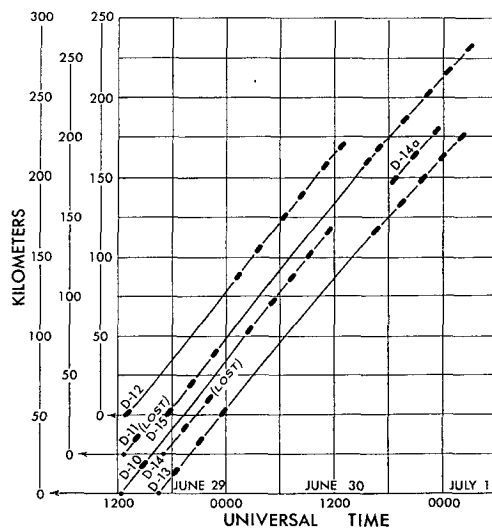

FIG. 2. Time-distance plot for all drogues. Initial slopes correspond to a drogue speed of 200 cm sec^{-1}, final slopes to 160 and 170 cm sec^{-1}.

TABLE 2. Neighbor diffusivity F.

Mean drogue separation, L_0 (km)	Number of drogue pairs	F (10^4 cm² sec⁻¹)	Degrees of freedom, n*	95% Confidence level** (10^4 cm² sec⁻¹)
3.9±0.3	161	19.3	18	11.0–42.4
2.2±0.2	90	3.7	13	3.9– 9.6

* With n drogues we have m drogue pairs according to $n(n-1)/2=m$. The n selected is the smaller of the two that bracket a given m.
** 95%, for a Chi-square probability distribution.

turbulence was both stationary and homogeneous. This allows us to imagine that a set of, say, 91 successive observations of drogue separations 10 min apart, as equivalent to a set of 14 drogues released simultaneously in the same small area and the separation of the resulting 91 drogue pairs measured also simultaneously 10 min later.

The data are divided into two groups, according to the range of separation; the larger range corresponds to the first ~ 24 hr of 161 successive observations, while the smaller range corresponds to the last 6 hr of 90 observations. The computed neighbor diffusivities are shown in Table 2, where the ratio of the large to the small F is seen to be 5.2 or about twice as large as would be expected from (1) when L is doubled. However, the confidence intervals for the F's are sufficiently broad to ascribe the apparent discrepancy to statistical randomness. In comparison with other studies, we find that Table 2 shows values larger than those proposed by Okubo (1968), but smaller than those proposed by Ichiye and Olson (1960).

In general, F contains contributions from many processes, some of which may not be stochastic and are
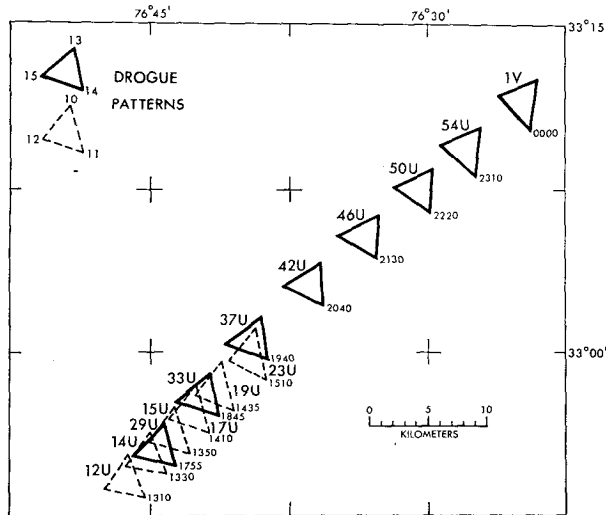

FIG. 3. Plan view of initial drogue drifts as a procession of triangles formed from selected drogue positions as vertices. Universal time is indicated on 29 June 1968.
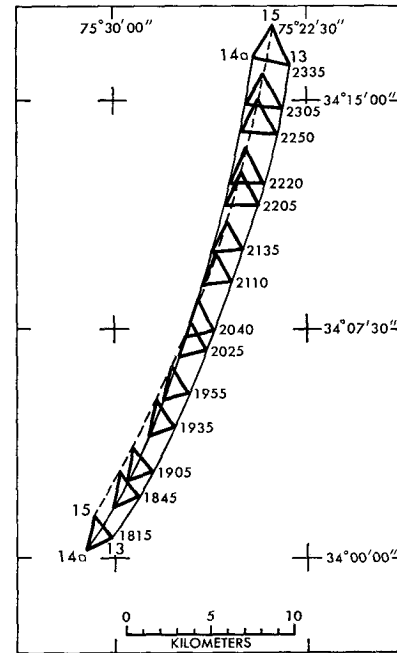

FIG. 4. Plan view of drogue drifts for drogues 13, 14a and 15 as a procession of triangles formed from selected drogue positions as vertices. An interesting feature is the crossing of the paths of drogues 14a and 15. Universal time is indicated on 30 June 1968.

governed by other than probabilistic law. To detect the presence of a nonstochastic component, we apply the trend test to the data presented in Fig. 5. For N observations of a random variable, where the observations are denoted by x_i, $i=1, 2, 3, \ldots, N$, we count the number of times that $x_i > x_j$, for $i < j$. Each such inequality is called a reverse arrangement and the total number is denoted by A. The test is a relatively powerful one for detecting a monotonic trend. We confine the test to the distance between drogues with the results summarized in Table 3. During the first 10 hr, two out of three drogue pairs underwent separations that are compatible with stochastic processes, particularly the drogue pairs oriented closest to the downstream direction of the current. However, during the last 6 hr, all

TABLE 3. Trend test for distance between drogue pairs.

Date	Time (GMT)	Drogue pair	N	A
29 June	1255–1510	10–11	12	8*
		12–10	12	27
		12–11	12	31
	1735–2350	13–14	31	151*
		14–15	31	220
		13–15	31	241
30 June	0110–1210	10–12	39	235*
	1815–0010	13–15	30	16*
		13–14a	30	77*
		14a–15	30	319*

* Indicates rejection, at the 2% level of significance, of the hypothesis that the series were independent observations of a random variable (see, e.g., Bendat and Piersol, 1966).

a. Drogues 10, 11 and 12.

b. Drogues 13, 14 and 15.

c. Drogues 10 and 12.
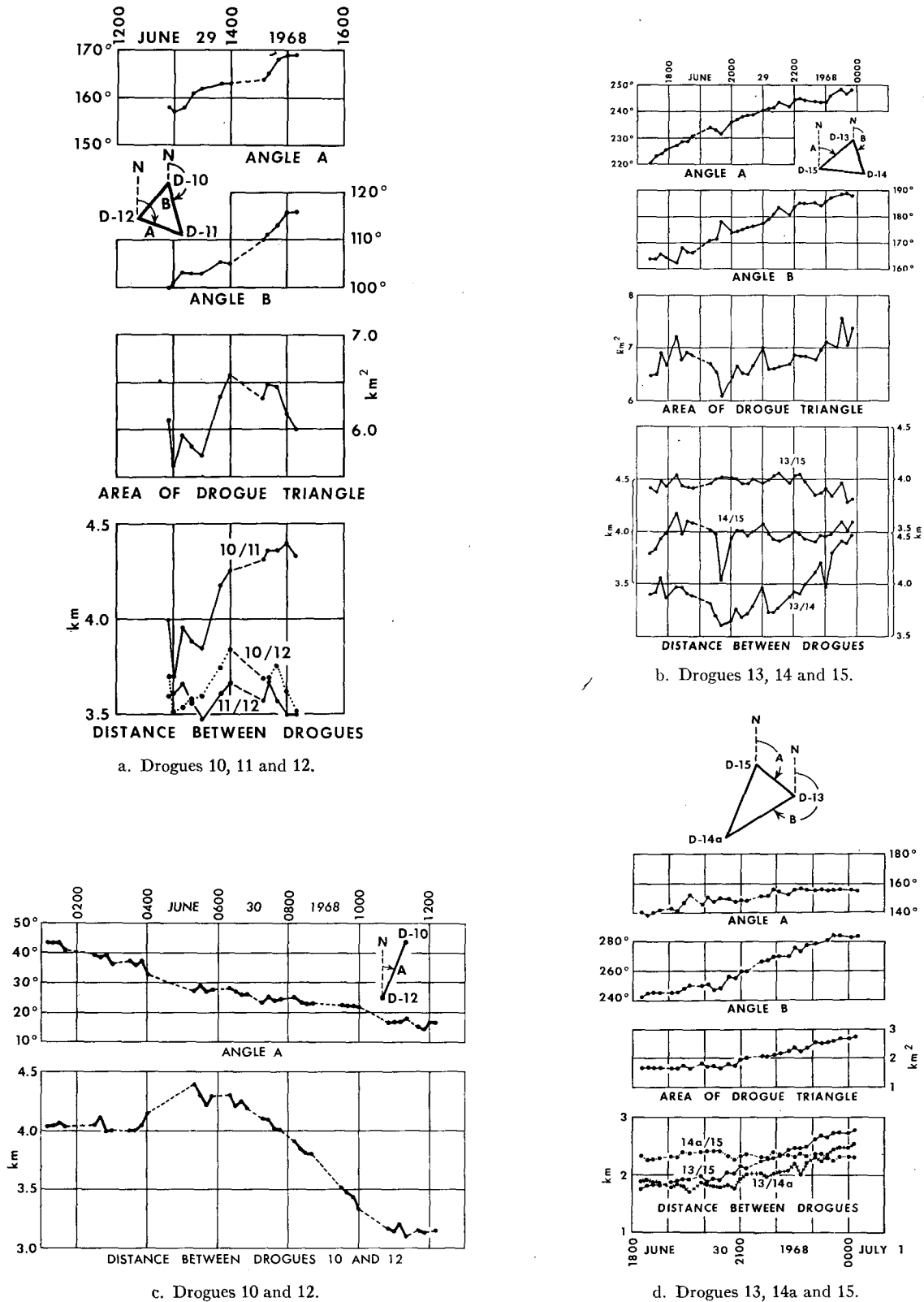
d. Drogues 13, 14a and 15.

FIG. 5. Observed separation between drogue pairs, orientation of lines joining drogue pairs, and area of resulting triangles. An especially noteworthy feature is the large change in the orientation and length of the line joining drogue pair 13 and 15 between sequences b and d.
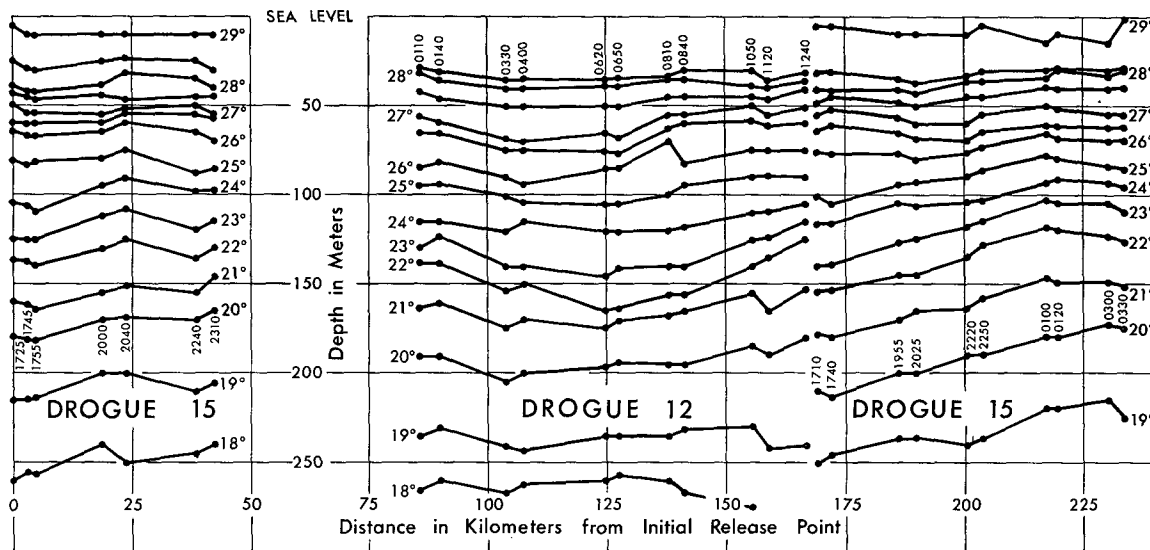
FIG. 6. Vertical temperature (°C) sections along paths of drogues 12 and 15. All soundings were made from same mechanical BT. Universal mean time began on 28 June and ended on 1 July 1968.

three drogue pairs underwent separations that are compatible only with non-stochastic processes. Generally, the overall situation was one of evolution toward a systematic trend.

5. Horizontal divergence

When there is no vertical shear in the horizontal velocity, the horizontal divergence D of a moving column is given by

$$D = (1/A)(dA/dt) = -(1/H)(dH/dt), \qquad (2)$$

where A is the horizontal area of a column of height H. Vertical shear is usually present in the current, but that related to baroclinicity in the region of the current away from the cyclonic flank is generally weaker (see Richardson et al., 1969). More pertinent to the present situation is the vertical shear associated with some of the many internal wave modes that are possible in a stratified fluid. The situation is simpler if a single inter-

nal wave mode predominates, as appears to have been the case during the last 6 hr. To see this, we view the temperature sections of Fig. 6 against the results of Table 3. The emergence of a definite trend in drogue separation implies a relative decline of stochastic processes and a concurrent rise of nonstochastic ones. Since the winds were light and the sea calm, the situation must be accompanied by a similar transition in the processes within the water. Turning to the temperature sequence in Fig. 6, we see undulations of the isotherms of many scales. But there is a tendency for a more readily recognizable pattern and a larger undulating amplitude in the lower isotherms as the tracking proceeded—a tendency matching the one for drogue separation. In the last temperature sequence, corresponding to the last set of three entries in Table 3, the field is dominated by the simultaneous and continuous rise of the 20–23C isotherms. From their respective initial depths, they rose in near unison to depths 30–35 m shallower. The evidence is fragmentary and inconclusive, but it is not incompatible with the suggestion of the arrival of a progressive, large-amplitude internal wave. In the progression of the wave, horizontal divergence is involved with a magnitude given by the right member in (2) if the vertical shear of horizontal motion is small. Hence, from the last sequence in Fig. 6, we find

$$D = -(1/H)(dH/dt) \approx (1/120\mathrm{m})$$
$$\times (35\mathrm{m}/6\mathrm{hr}) = 1.4 \times 10^{-5}\ \mathrm{sec}^{-1}. \qquad (3)$$

While from Fig. 5d, with some smoothing of the time-area plot, we have

$$D = (1/A)(dA/dt) \approx (1/2.2\mathrm{km}^2)(1\mathrm{km}^2/6\mathrm{hr})$$
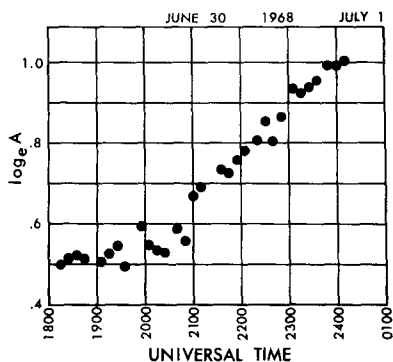$$\approx 2.1(\pm 0.5) \times 10^{-5}\ \mathrm{sec}^{-1}. \qquad (4)$$

FIG. 7. Plot of the natural logarithm of the area of the triangles depicted in Fig. 4 vs time. The zero of the ordinate starts at 23.03 corresponding to the natural logarithm of 1 km².

These independent estimates are in agreement, for the difference may be reasonably ascribed to errors introduced when we extended horizontal divergence, actually a point property of the fluid, to situations covering areas and volumes.

6. Discussion

The horizontal divergence D affects the neighbor diffusivity F. An estimate of the order of magnitude of this effect is direct, if the square of the drogue separation L is proportional to the area A. For this purpose, we consider D a constant for the period in order to obtain from the left two members of (2) the expression

$$A = A_0 e^{Dt}, \tag{5}$$

a growth that is supported by the plot in Fig. 7 of the natural logarithm of the area against time. Thus, replacing A and A_0 in (5) by L^2 and L_0^2, we have from (1)

$$F = BL^{\frac{4}{3}} \approx BL_0^{\frac{4}{3}}(e^{Dt})^{\frac{2}{3}} = 4 \times 10^4 \text{ cm}^2 \text{ sec}^{-1}, \tag{6}$$

for $B = 1/400$, D as in (4), $L_0 = 2$ km, and $t = 6$ hr. Unless B is substantially smaller, we may conclude that the magnitude of F for the last 6 hr was due primarily to the process of horizontal divergence.

The progression of a wave is accompanied by horizontal divergence. If the divergence (4) is so related, the features of the responsible wave appear to share some of the characteristics of the Sverdrup wave, in the terminology of Veronis and Stommel (1955). On the basis of the 6 hr taken for the drogues to cover an apparent wavelength of 50 km, these features have a wavelength of the order of 200 km and a tidal or near-inertial frequency.

When long, internal waves of near-inertial frequency are present in the Gulf Stream, interaction between them appears likely. One aspect is the direct effect of the horizontal divergence of the wave on the relative vorticity of the current; we consider this briefly. Neglecting both the friction and solenoid terms, and writing f for the Coriolis parameter, the equation for time change in the vertical component of relative vorticity ζ of a moving column is

$$d\zeta/dt \doteq -(\zeta + f)D - \mathbf{V} \cdot \nabla f, \tag{7}$$

where all vectors are horizontal. We can evaluate ζ from the observed data that went into the illustration in Fig. 4. Using natural coordinates, with the curvature and shear terms having opposite signs in the present case, we have

$$\zeta = KV - (\partial V/\partial n) \approx (170 \text{ cm sec}^{-1}/85 \text{ km})$$
$$- (5 \text{ cm sec}^{-1}/1.5 \text{ km}) \approx -1 \times 10^{-5} \text{ sec}^{-1}. \tag{8}$$

Consequently, the first term in the second member of (7) is of the magnitude

$$-(f + \zeta)D \approx -(7 \times 10^{-5})(1.7 \times 10^{-5})$$
$$\approx -120 \times 10^{-11} \text{ sec}^{-2} \tag{9}$$

for $f = 8 \times 10^{-5}$ sec^{-1}, and D taken as the average of (3) and (4). The latitudinal change in the Coriolis parameter, important in the model of Warren (1963), is at most, in the present case, of the magnitude of $(170 \text{ cm sec}^{-1})(2 \times 10^{-13} \text{ cm}^{-1} \text{ sec}^{-1}) = 3.4 \times 10^{-11} \text{ sec}^{-2}$. Hence, in 6.5 hr, the amount of negative relative vorticity gained by the column is

$$(-120 + 3.4) \times 10^{-11} \times 2.35 \times 10^4 = -2.7 \times 10^{-5} \text{ sec}^{-1},$$

or one-third of the local magnitude of f. As the latitudinal change in f is small in comparison, Eq. (7) may be reduced to

$$(f_0 + \zeta)A = \text{constant}, \tag{10}$$

where f_0 is a constant. The application of (10) to a portion of the Gulf Stream system was anticipated by Stommel (1953) who discussed the effect of the constriction of the Florida Channel on the relative vorticity of the Florida Current.

7. Conclusion

We have shown, on favorable occasions, that it is feasible to measure horizontal divergence on a scale relevant to potential vorticity conservation on an f plane. In this instance, the mechanism responsible for the divergence appears related to a large-amplitude, long internal wave of tidal or near-inertial frequency.

REFERENCES

Bendat, J. S., and A. G. Piersol, 1966: *Measurement and Analysis of Random Data.* New York, Wiley, 390 pp.

Chew, Frank, and G. A. Berberian, 1970: Some measurements by shallow drogues in the Florida Current. *Limnol. Oceanog.,* 15, 88–99.

Ichiye, R., and F. C. W. Olson, 1960: On neighbor diffusivity in the ocean. *Deut. Hydrog. Z.,* 13, 13–23.

Newton, C. W., 1961: Estimates of vertical motions and meridional heat exchange in Gulf Stream eddies, and a comparison with atmospheric disturbances. *J. Geophys. Res.,* 66, 853–870.

Niiler, P. P., 1969: On the Ekman divergence in an oceanic jet. *J. Geophys. Res.,* 74, 7048–7052.

Okubo, A., 1962: A review of theoretical models for turbulent diffusion in the sea. *J. Oceanogr. Soc. Japan,* 20th Anniv. Vol., 286–320.

——, 1968: A new set of oceanic diffusion diagrams. Chesapeake Bay Inst., Tech. Rept. 38, 35 pp.

Richardson, W. S., W. J. Schmitz and P. P. Niiler, 1969: The velocity structure of the Florida Current from the Straits of Florida to Cape Fear. *Deep-Sea Res.,* 16, 225–231.

Stommel, 1949: Horizontal diffusion due to oceanic turbulence. *J. Marine Res.,* 8, 199–225.

——, 1953: Examples of the possible role of inertia and stratification in the dynamics of the Gulf Stream system. *J. Marine Res.,* 12, 184–195.

Veronis, G., and H. Stommel, 1955: The action of variable wind stresses on a stratified ocean. *J. Marine Res.,* 15, 43–75.

Warren, B. A., 1963: Topographic influence on the path of the Gulf Stream. *Tellus,* 15, 167–183.